

Effect of the $K\bar{K}$ and $\eta\eta$ channels and interference phenomena in the two-pion and $K\bar{K}$ transitions of charmonia and bottomonia

Yury S. Surovtsev,¹ Petr Bydžovský,² Thomas Gutsche,^{3,4} Robert Kamiński,⁴
Valery E. Lyubovitskij,^{3,5,6,7} and Miroslav Nagy⁸

¹*Bogoliubov Laboratory of Theoretical Physics, Joint Institute for Nuclear Research, 141980 Dubna, Russia*

²*Nuclear Physics Institute of the AS CR, 25068 Řež, Czech Republic*

³*Institut für Theoretische Physik, Universität Tübingen, Kepler Center for Astro and Particle Physics, Auf der Morgenstelle 14, D-72076 Tübingen, Germany*

⁴*Institute of Nuclear Physics PAS, Cracow 31342, Poland*

⁵*Departamento de Física y Centro Científico Tecnológico de Valparaíso-CCTVal, Universidad Técnica Federico Santa María, Casilla 110-V Valparaíso, Chile*

⁶*Department of Physics, Tomsk State University, 634050 Tomsk, Russia*

⁷*Laboratory of Particle Physics, Tomsk Polytechnic University, 634050 Tomsk, Russia*

⁸*Institute of Physics, SAS, Bratislava 84511, Slovak Republic*



(Received 3 October 2017; published 22 January 2018)

It is shown that the basic shape of dipion and $K\bar{K}$ mass spectra in decays $J/\psi \rightarrow \phi(\pi\pi, K\bar{K})$, $\psi(2S) \rightarrow J/\psi\pi\pi$, $Y(4260) \rightarrow J/\psi\pi\pi$ and in the two-pion transitions of bottomonia states are explained by an unified mechanism based on the contribution of the $\pi\pi$, $K\bar{K}$ and $\eta\eta$ coupled channels including their interference. The role of the individual f_0 resonances in making up the shape of the dipion mass distributions in the charmonia and bottomonia decays is considered.

DOI: [10.1103/PhysRevD.97.014009](https://doi.org/10.1103/PhysRevD.97.014009)

I. INTRODUCTION

The last years achievements of the hadron spectroscopy are related mainly to heavy mesons including charmonia and bottomonia. Therefore, of course, there is a problem of studying structure of these mesons and their interaction for exploring nonperturbative QCD. There were expressed thoughts that for these aims the two-pion transitions of bottomonia are suitable (see, e.g., [1] and references therein). Clearly, first it is necessary to allow for the final-state interaction in decays of bottomonia. When studying processes $Y(mS) \rightarrow Y(nS)\pi\pi$, the $\pi\pi$ interaction should be considered with taking into account the coupled channels, whereas the final vector meson $Y(nS)$ remains a spectator.

In Refs. [2,3], devoted to explanation of the two-pion transitions of bottomonia, we have shown that the basic shape of dipion mass spectra in the decays both of bottomonia and charmonia are explained by the unified mechanism which is based on our previous conclusions on wide resonances [4,5] and is related to contributions of the $\pi\pi$ and $K\bar{K}$ coupled channels including their interference and allowing for our

earlier results on the explanation of charmonia decays $J/\psi \rightarrow \phi(\pi\pi, K\bar{K})$ and $\psi(2S) \rightarrow J/\psi(\pi\pi)$ [6,7]. In indicated decays pseudoscalar meson pairs are produced mainly in the scalar-isoscalar state. In Refs. [4,5] it was shown that correct parameters of the f_0 mesons cannot be obtained when studying only the $\pi\pi$ scattering. Allowance for the coupled $K\bar{K}$ channel and consideration of the corresponding experimental data improve situation. However, in order to extract more correct values of the f_0 parameters it is needed to take into account also the coupled $\eta\eta$ channel. Note that here talking must be about the combined analysis of data on the isoscalar S-wave processes $\pi\pi \rightarrow \pi\pi, K\bar{K}, \eta\eta$, of accessible data on the charmonia decay processes— $J/\psi \rightarrow \phi(\pi\pi, K\bar{K})$, $\psi(2S) \rightarrow J/\psi\pi\pi$ (Crystal Ball [8], DM2 [9], Mark II [10], Mark III [11], and BES II [12] Collaborations) and of practically all available data on two-pion transitions of the Y mesons from the ARGUS [13], CLEO [14], CUSB [15], Crystal Ball [16], Belle [17], and BABAR [18] Collaborations— $Y(mS) \rightarrow Y(nS)\pi\pi$ ($m > n$, $m = 2, 3, 4, 5$, $n = 1, 2, 3$).

When analyzing the charmonia and bottomonia decays with allowing for also the $\eta\eta$ channel, we need to include the $\pi\pi \rightarrow \eta\eta$ and $K\bar{K} \rightarrow \eta\eta$ amplitudes, respectively. In the former case the phase shift of $\pi\pi \rightarrow \eta\eta$ amplitude is unknown from data, in the latter the $K\bar{K} \rightarrow \eta\eta$ amplitude is experimentally unknown entirely. However, thanks to the Le Couteur–Newton relations [19], which represent all

Published by the American Physical Society under the terms of the [Creative Commons Attribution 4.0 International license](https://creativecommons.org/licenses/by/4.0/). Further distribution of this work must maintain attribution to the author(s) and the published article's title, journal citation, and DOI. Funded by SCOAP³.

amplitudes of transitions between three coupled channels ($\pi\pi$, $K\bar{K}$ and $\eta\eta$) via one function—the Jost matrix determinant, we know the model-independent part of the amplitude related to resonances. The only remaining important problem is the description of the background part. After solution of this problem we shall be able to predict the unknown indicated amplitudes.

Thus, the main aim of this investigation is to prolong the study of scalar meson properties analyzing jointly data on the isoscalar S-wave processes $\pi\pi \rightarrow \pi\pi$, $K\bar{K}$, $\eta\eta$, on charmonia decays— $J/\psi \rightarrow \phi(\pi\pi, K\bar{K})$, $\psi(2S) \rightarrow J/\psi\pi\pi$ and $Y(4260) \rightarrow J/\psi\pi\pi$ and on the above-indicated two-pion transitions of bottomonia. This task is timely in view of that is very important. However, up to now it is not completely carried out. For e.g., analyzing the multichannel $\pi\pi$ scattering and the decays $J/\psi \rightarrow \phi(\pi\pi, K\bar{K})$ with the data of Mark III and DM2 Collaborations in the framework of our approach based on analyticity and unitarity and with using an uniformization procedure, we have obtained parameters of the $f_0(600)$ and $f_0(1500)$ which differ considerably from results of analyses based on some other methods (mainly those based on the dispersion relations and Breit-Wigner approaches) [20,21]. Moreover, it was found that the data admit two sets of parameters of $f_0(500)$ with a mass relatively near to the ρ -meson mass, and with the total widths either ≈ 600 or ≈ 930 MeV. Addition to the combined analysis the BES II data on $J/\psi \rightarrow \phi\pi\pi$ has given the important result choosing surely from two solutions for the $f_0(500)$ the one with the larger width [6]. When expanding the analysis via adding the data on decays $\psi(2S) \rightarrow J/\psi\pi\pi$ and on the two-pion transitions of bottomonia, the satisfactory description did not require the alteration of the f_0 parameters, thus confirming our earlier conclusions about the scalar-isoscalar mesons. Also there was obtained the interesting and unified explanation of dipion mass spectra for the indicated charmonia and bottomonia decays [2,3]. For e.g., we have showed that the experimentally observed interesting behavior of the $\pi\pi$ spectra of the Y -family decays, beginning from the second radial excitation and higher—a bell-shaped form in the near- $\pi\pi$ -threshold region, smooth dips about 0.6 GeV in the $Y(4S, 5S) \rightarrow Y(1S)\pi^+\pi^-$, about 0.45 GeV in the $Y(4S, 5S) \rightarrow Y(2S)\pi^+\pi^-$, and about 0.7 GeV in the $Y(3S) \rightarrow Y(1S)(\pi^+\pi^-, \pi^0\pi^0)$, and also sharp dips about 1 GeV in the $Y(4S, 5S) \rightarrow Y(1S)\pi^+\pi^-$ —is explained by the interference between the $\pi\pi$ scattering and $K\bar{K} \rightarrow \pi\pi$

contributions to the final states of these decays (by the constructive one in the near- $\pi\pi$ -threshold region and by the destructive one in the dip regions).

Clearly, the allowance for effect of the $\eta\eta$ channel in the indicated two-pion transitions (as of the $\pi\pi$ and $K\bar{K}$ channels) not only kinematically (i.e., taking account the channel threshold via the uniformizing variable) and also by adding the $\pi\pi \rightarrow \eta\eta$ amplitude in the corresponding formulas for the decays permit us to extend description of the $\pi\pi$ spectra of relevant decays above the $\eta\eta$ threshold. Besides specifying the decay parameters, we are going to clarify a role of individual resonances.

II. THE EFFECT OF MULTICHANNEL $\pi\pi$ SCATTERING IN DECAYS OF THE ψ - AND Y -MESON FAMILIES

Considering multichannel $\pi\pi$ scattering, we shall deal with the 3-channel case, i.e., with the reactions $\pi\pi \rightarrow \pi\pi, K\bar{K}, \eta\eta$, because it was shown [5] that this is a minimal number of coupled channels needed for obtaining correct values of f_0 -resonance parameters. When performing our combined analysis data for the multichannel $\pi\pi$ scattering were taken from many papers (see Refs. in our paper [6]). For the decay $J/\psi \rightarrow \phi\pi^+\pi^-$ data were taken from Mark III, DM2 and BES II Collaborations; for $\psi(2S) \rightarrow J/\psi(\pi^+\pi^-$ and $\pi^0\pi^0)$ —from Mark II and Crystal Ball(80) (see Refs. also in [6]). For $Y(2S) \rightarrow Y(1S)(\pi^+\pi^-$ and $\pi^0\pi^0)$ data were used from ARGUS [13], CLEO [14], CUSB [15], and Crystal Ball [16] Collaborations; for $Y(3S) \rightarrow Y(1S)(\pi^+\pi^-$, $\pi^0\pi^0)$ and $Y(3S) \rightarrow Y(2S)(\pi^+\pi^-, \pi^0\pi^0)$ —from CLEO [22,23]; for $Y(4S) \rightarrow Y(1S, 2S)\pi^+\pi^-$ —from BABAR [18] and Belle [17]; for $Y(5S) \rightarrow Y(1S, 2S, 3S)(\pi^+\pi^-, \pi^0\pi^0)$ —from Belle Collaboration [17,24].

The used formalism for calculating the dimeson mass distributions in the quarkonia decays is analogous to the one proposed in Ref. [25] for the decays $J/\psi \rightarrow \phi(\pi\pi, K\bar{K})$ and $V' \rightarrow V\pi\pi$ ($V = \psi, Y$) but with allowing for also amplitudes of transitions between the $\pi\pi$, $K\bar{K}$ and $\eta\eta$ channels in decay formulas. There was assumed that the meson pairs in the final state have zero isospin and spin. Only these pairs of mesons undergo final state interactions whereas the final $Y(nS)$ meson ($n < m$) remains a spectator. The amplitudes of decays are related with the scattering amplitudes T_{ij} ($i, j = 1 - \pi\pi, 2 - K\bar{K}, 3 - \eta\eta$) as follows

$$F(J/\psi \rightarrow \phi\pi\pi) = \frac{1}{\sqrt{3}} \left[c_1(s)T_{11} + \left(\frac{\alpha_2}{s - \beta_2} + c_2(s) \right) T_{12} + c_3(s)T_{13} \right], \quad (1)$$

$$F(J/\psi \rightarrow \phi K\bar{K}) = \frac{1}{\sqrt{2}} [c_1(s)T_{21} + c_2(s)T_{22} + c_3(s)T_{23}], \quad (2)$$

$$F(\psi(2S) \rightarrow \psi(1S)\pi\pi) = \frac{1}{\sqrt{3}} [d_1(s)T_{11} + d_2(s)T_{12} + d_3(s)T_{13}], \quad (3)$$

$$F(Y(mS) \rightarrow Y(nS)\pi\pi) = \frac{1}{\sqrt{3}} [e_1^{(mn)}T_{11} + e_2^{(mn)}T_{12} + e_3^{(mn)}T_{13}], \quad (4)$$

$$m > n, \quad m = 2, 3, 4, 5, \quad n = 1, 2, 3$$

where $c_i = \gamma_{i0} + \gamma_{i1}s$, $d_i = \delta_{i0} + \delta_{i1}s$ and $e_i^{(mn)} = \rho_{i0}^{(mn)} + \rho_{i1}^{(mn)}s$; indices m and n correspond to $\Upsilon(mS)$ and $\Upsilon(nS)$, respectively. The free parameters α_2 , β_2 , γ_{i0} , γ_{i1} , δ_{i0} , δ_{i1} , $\rho_{i0}^{(mn)}$ and $\rho_{i1}^{(mn)}$ depend on the couplings of J/ψ , $\psi(2S)$ and the $\Upsilon(mS)$ to the channels $\pi\pi$, $K\bar{K}$ and $\eta\eta$. The pole term in Eq. (1) in front of T_{12} is an approximation of possible ϕK states, not forbidden by Okubo-Zweig-Iizuka (OZI) rules. Generally, considering quark diagrams, one can see that due to the OZI rules it ought to introduce the pole term in Eq. (2) in front of T_{22} . However it is turned out that this pole even a little deteriorates the description. Therefore, it is excluded from Eq. (2). The numbers in front of square brackets are coefficients of the vector addition of two isospins $I^{(1)}$ and $I^{(2)}$ ($I^{(1)}I^{(2)}I_3^{(1)}I_3^{(2)}|II_3$) where I and I_3 are the total isospin and its third component. These coefficients are distinct from zero if $I_3 = I_3^{(1)} + I_3^{(2)}$. The explicit form of relevant coefficient of the vector addition is

$$(I^{(1)}I^{(2)}I_3^{(1)}, -I_3^{(1)}|00) = (-1)^{I^{(2)}-I_3^{(1)}} \frac{\delta_{I^{(1)}I^{(2)}}}{\sqrt{2I^{(2)}+1}}. \quad (5)$$

Then inserting the numerical values of pion and kaon isospins, we obtain the corresponding coefficients in Eqs. (1)–(4).

The amplitudes T_{ij} are expressed through the S -matrix elements

$$S_{ij} = \delta_{ij} + 2i\sqrt{\rho_1\rho_2}T_{ij} \quad (6)$$

where $\rho_i = \sqrt{1 - s_i/s}$ and s_i is the reaction threshold. The S -matrix elements are taken as the products

$$S = S^{\text{bgr}}S^{\text{res}} \quad (7)$$

where S^{res} represents the contribution of resonances, S^{bgr} is the background part. The S^{res} -matrix elements are parametrized on the uniformization plane of the $\pi\pi$ -scattering S -matrix element by poles and zeros which represent resonances. The uniformization plane is obtained by a conformal map of the 8-sheeted Riemann surface, on which the three-channel S matrix is determined, onto the plane. In the uniformizing variable used [20]

$$w = \frac{\sqrt{(s-s_2)s_3} + \sqrt{(s-s_3)s_2}}{\sqrt{s(s_3-s_2)}} \quad (8)$$

$$(s_2 = 4m_K^2 \quad \text{and} \quad s_3 = 4m_\eta^2)$$

we have neglected the $\pi\pi$ -threshold branch point and allowed for the $K\bar{K}$ - and $\eta\eta$ -threshold branch points and left-hand branch point at $s = 0$ related to the crossed channels. Reason of neglecting the $\pi\pi$ -threshold branch point consists in following. With the help of a simple mapping, a function, determined on the 8-sheeted Riemann surface, can be

uniformized only on torus. This is unsatisfactory for our purpose. Therefore, we neglect the influence of the lowest ($\pi\pi$) threshold branch-point (however, unitarity on the $\pi\pi$ -cut is taken into account). An approximation like this means the consideration of the nearest to the physical region semi-sheets of the Riemann surface of the S -matrix. In fact, we construct a 4-sheeted model of the initial 8-sheeted Riemann surface approximating it in accordance with our approach of a consistent account of the nearest singularities on all the relevant sheets. In practice the disregard of influence of the $\pi\pi$ -threshold branch-point denotes that we do not describe some small region near the threshold. This problem was discussed with some details in our earlier works, e.g., in [20].

Resonance representations on the Riemann surface are obtained using formulas from Ref. [26], expressing analytic continuations of the S -matrix elements to all sheets in terms of those on the physical (I) sheet that have only the resonances zeros (beyond the real axis), at least, around the physical region. These formulas show how singularities and resonance poles and zeros are transferred from the matrix element S_{11} to matrix elements of coupled processes.

The background is introduced to the S^{bgr} -matrix elements in a natural way: on the threshold of each important channel there appears generally speaking a complex phase shift. It is important that we have obtained practically zero background of the $\pi\pi$ scattering in the scalar-isoscalar channel. This confirms well, first, our assumption $S = S^{\text{bgr}}S^{\text{res}}$. Since in the following combined analysis of the multichannel $\pi\pi$ scattering, of the decays $J/\psi \rightarrow \phi(\pi\pi, K\bar{K})$, $\psi(2S) \rightarrow J/\psi\pi\pi$, $Y(4260) \rightarrow J/\psi\pi\pi$ and of the two-pion transitions of bottomonia state we were not forced to change the resonance-pole positions on the Riemann surface of the S -matrix and the background parameters, we do not give here their values which can be found in other our papers (e.g., in Ref. [6]).

Generally, *wide multichannel states are most adequately represented by poles*, because the poles give the main model-independent effect of resonances and are rather stable characteristics for various models, whereas masses and total widths are very model-dependent for wide resonances [27]. The latter and coupling constants of resonances with channels should be calculated using the poles on sheets II, IV, and VIII, because only on these sheets the analytic continuations have the forms:

$$\propto 1/S_{11}^I, \quad \propto 1/S_{22}^I \quad \text{and} \quad \propto 1/S_{33}^I,$$

respectively, i.e., the pole positions of resonances are at the same points of the complex-energy plane, as the resonance zeros on the physical sheet, and are not shifted due to the coupling of channels.

Further, since studying the decays of charmonia and bottomonia, we investigated the role of the individual f_0 resonances in contributing to the shape of the dipion mass distributions in these decays, firstly we studied their role in

forming the energy dependence of amplitudes of reactions $\pi\pi \rightarrow \pi\pi, K\bar{K}, \eta\eta$. In this case we switched off only those resonances [$f_0(500)$, $f_0(1370)$, $f_0(1500)$ and $f_0(1710)$], removal of which can be somehow compensated by correcting the background (maybe, with elements of the pseudobackground) to have the more-or-less acceptable description of the multichannel $\pi\pi$ scattering. Therefore, below we considered the description of the multichannel $\pi\pi$ scattering more for two cases [3]:

- (i) first, when leaving out a minimal set of the f_0 mesons consisting of the $f_0(500)$, $f_0(980)$, and $f'_0(1500)$, which is sufficient to achieve a description of the processes $\pi\pi \rightarrow \pi\pi, K\bar{K}, \eta\eta$ with a total $\chi^2/\text{ndf} \approx 1.20$.
- (ii) Second, from above-indicated three mesons only the $f_0(500)$ can be switched off while still obtaining a reasonable description of multichannel $\pi\pi$ scattering (though with an appearance of the pseudobackground) with a total $\chi^2/\text{ndf} \approx 1.43$.

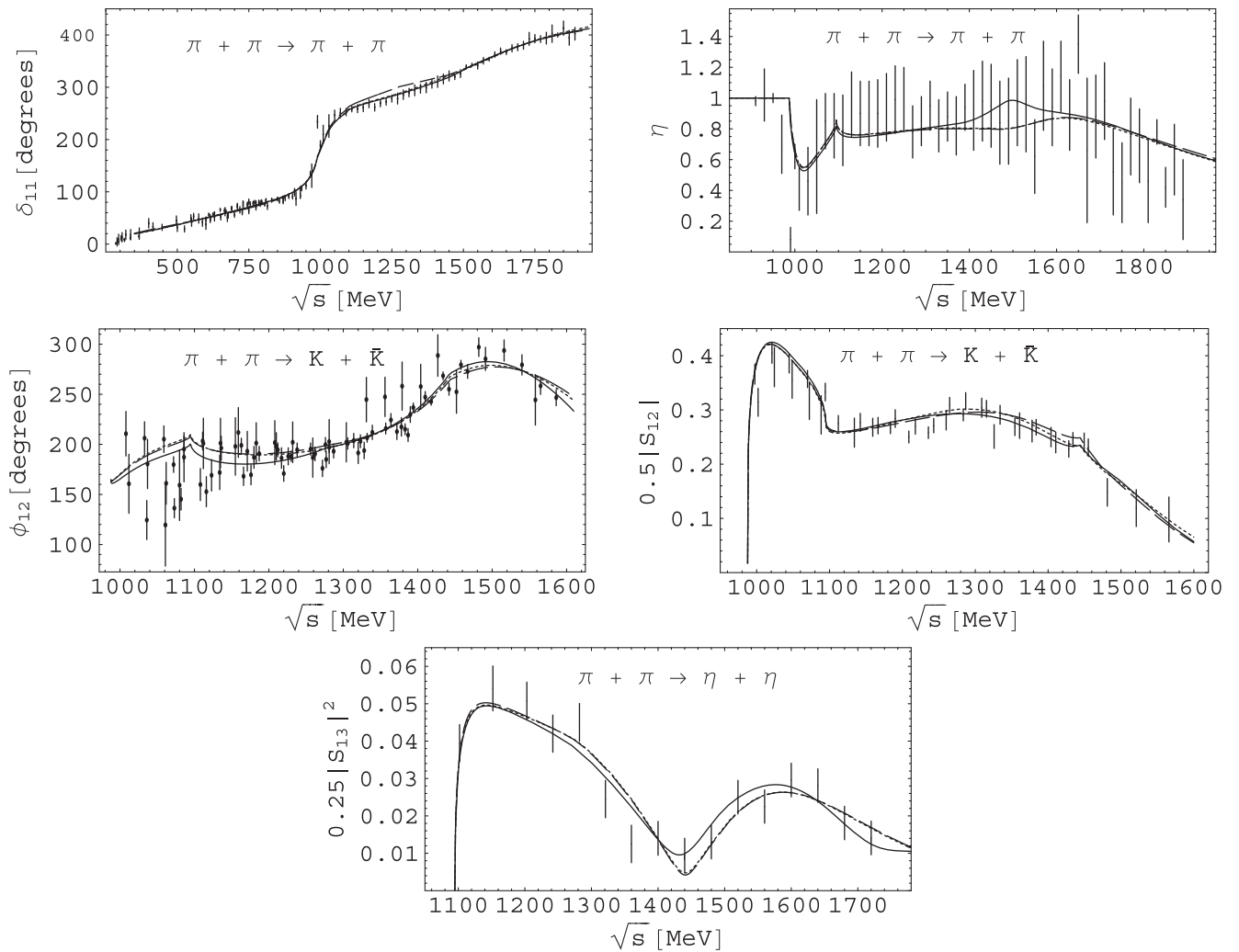


FIG. 1. The phase shifts and moduli of the S -matrix element in the S -wave $\pi\pi$ -scattering (upper panel), in $\pi\pi \rightarrow K\bar{K}$ (middle panel), and the squared modulus of the $\pi\pi \rightarrow \eta\eta$ S -matrix element (lower figure). The solid lines correspond to contribution of all relevant f_0 -resonances; the dotted, of the $f_0(500)$, $f_0(980)$, and $f'_0(1500)$; the dashed, of the $f_0(980)$ and $f'_0(1500)$.

In Fig. 1 we show the obtained description of the processes $\pi\pi \rightarrow \pi\pi, K\bar{K}, \eta\eta$. The solid lines correspond to contribution of all relevant f_0 -resonances; the dotted, of the $f_0(500)$, $f_0(980)$, and $f'_0(1500)$; the dashed, of the $f_0(980)$ and $f'_0(1500)$. One can see that the curves are quite similar in all three cases.

Coming back to the decay analysis, the expression

$$N|F|^2 \sqrt{(s-s_1)[m_\psi^2 - (\sqrt{s}-m_\phi)^2][m_\psi^2 - (\sqrt{s}+m_\phi)^2]} \quad (9)$$

for decays $J/\psi \rightarrow \phi(\pi\pi, K\bar{K})$ and the analogues relations for $\psi(2S) \rightarrow \psi(1S)\pi\pi$ and $\Upsilon(mS) \rightarrow \Upsilon(nS)\pi\pi$ give the dimeson mass distributions. N (normalization to experiment) is: for $J/\psi \rightarrow \phi(\pi\pi, K\bar{K})$ 1.6663 (Mark III), 0.5645 (DM 2) and 12.1066 (BES II); for $\psi(2S) \rightarrow J/\psi\pi^+\pi^-$ 4.1763 (Mark II); for $\psi(2S) \rightarrow J/\psi\pi^0\pi^0$ 3.9825 (Crystal Ball(80)); for $\Upsilon(2S) \rightarrow \Upsilon(1S)\pi^+\pi^-$ 11.1938 (ARGUS), 5.6081 (CLEO

(94)) and 2.9249 (CUSB); for $\Upsilon(2S) \rightarrow \Upsilon(1S)\pi^0\pi^0$ 0.6627 (CLEO(07)) and 0.2071 (Crystal Ball(85)); for $\Upsilon(3S) \rightarrow \Upsilon(1S)(\pi^+\pi^- \text{ and } \pi^0\pi^0)$ 57.8466 and 13.1958 (CLEO(07)); for $\Upsilon(3S) \rightarrow \Upsilon(2S)(\pi^+\pi^- \text{ and } \pi^0\pi^0)$ 6.0706 and 4.1026 (CLEO(94)); for $\Upsilon(4S) \rightarrow \Upsilon(1S)\pi^+\pi^-$ 13.6322 (BABAR(06)) and 1.0588 (Belle(07)); for $\Upsilon(4S) \rightarrow \Upsilon(2S)\pi^+\pi^-$ 111.418 (BABAR(06)); for $\Upsilon(5S) \rightarrow \Upsilon(1S)\pi^+\pi^-$, $\Upsilon(5S) \rightarrow \Upsilon(2S)\pi^+\pi^-$ and $\Upsilon(5S) \rightarrow \Upsilon(3S)\pi^+\pi^-$ respectively 0.6258, 9.1608 and 20.0786 (Belle(12)); for $\Upsilon(5S) \rightarrow \Upsilon(1S)\pi^0\pi^0$, $\Upsilon(5S) \rightarrow \Upsilon(2S)\pi^0\pi^0$ and $\Upsilon(5S) \rightarrow \Upsilon(3S)\pi^0\pi^0$ respectively 0.2929, 3.0295, and 6.3207 (Belle(13)).

Satisfactory combined description of all considered processes is obtained with the total $\chi^2/\text{ndf}=842.958/(808-122)\approx 1.23$; for the $\pi\pi$ scattering, $\chi^2/\text{ndf}\approx 1.14$; for $\pi\pi \rightarrow K\bar{K}$, $\chi^2/\text{ndf}\approx 1.65$; for $\pi\pi \rightarrow \eta\eta$, $\chi^2/\text{ndf}\approx 0.88$; for decays $J/\psi \rightarrow \phi(\pi^+\pi^-, K\bar{K})$, $\chi^2/\text{ndf}\approx 1.26$ for $\psi(2S) \rightarrow J/\psi(\pi^+\pi^-, \pi^0\pi^0)$, $\chi^2/\text{ndf}\approx 2.74$; for $\Upsilon(2S) \rightarrow \Upsilon(1S)(\pi^+\pi^-, \pi^0\pi^0)$, $\chi^2/\text{ndf}\approx 1.07$; for $\Upsilon(3S) \rightarrow \Upsilon(1S)(\pi^+\pi^-, \pi^0\pi^0)$, $\chi^2/\text{ndf}\approx 1.08$, for $\Upsilon(3S) \rightarrow \Upsilon(2S)(\pi^+\pi^-, \pi^0\pi^0)$, $\chi^2/\text{ndf}\approx 0.71$, for $\Upsilon(4S) \rightarrow \Upsilon(1S)\times(\pi^+\pi^-)$, $\chi^2/\text{ndf}\approx 0.46$, for $\Upsilon(4S) \rightarrow \Upsilon(2S)(\pi^+\pi^-)$, $\chi^2/\text{ndf}\approx 0.20$, for $\Upsilon(5S) \rightarrow \Upsilon(1S)(\pi^+\pi^-, \pi^0\pi^0)$, $\chi^2/\text{ndf}\approx$

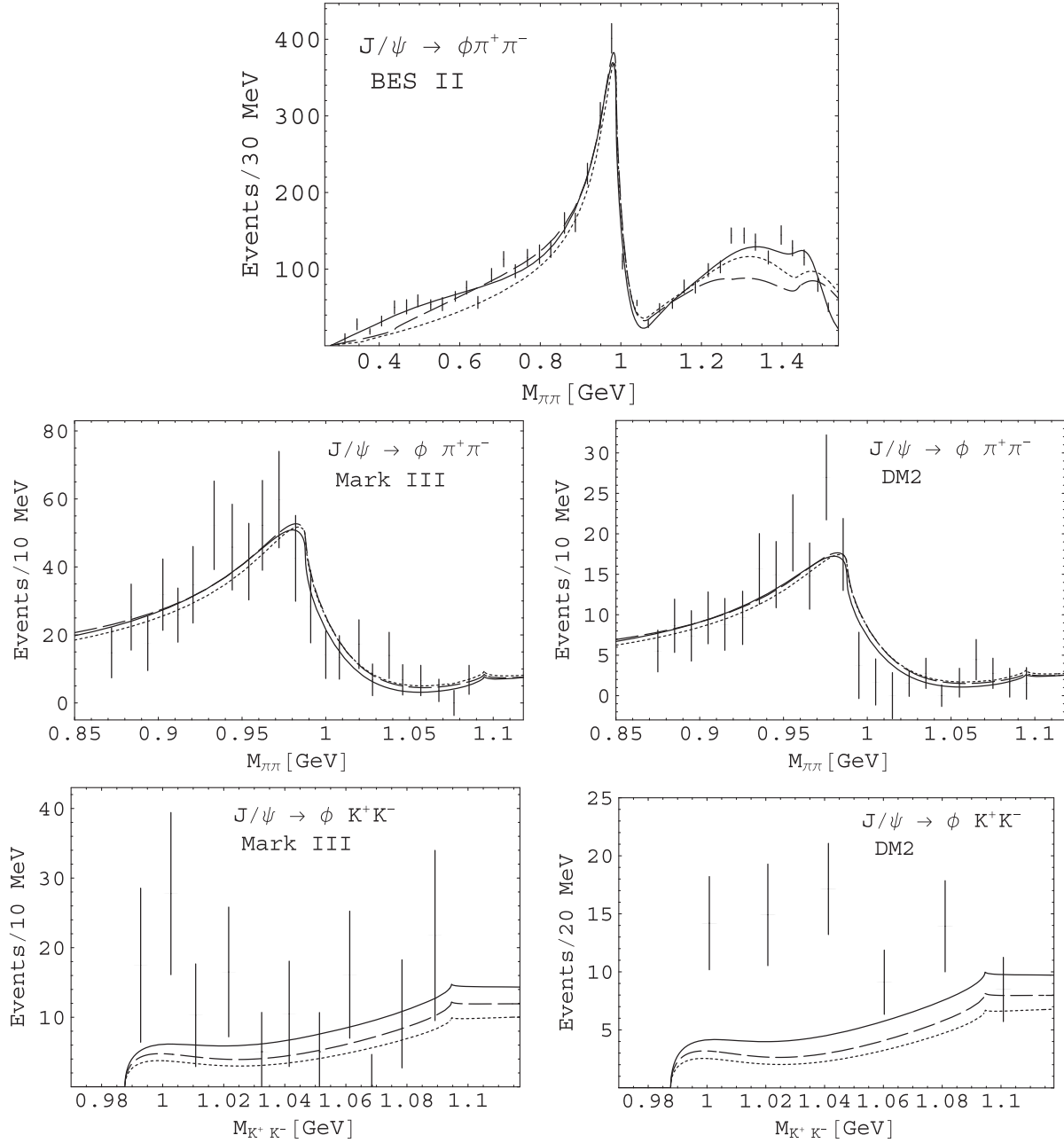


FIG. 2. The decays $J/\psi \rightarrow \phi(\pi^+\pi^-, K^+K^-)$. The solid, dotted and dashed lines as explained in Fig. 1.

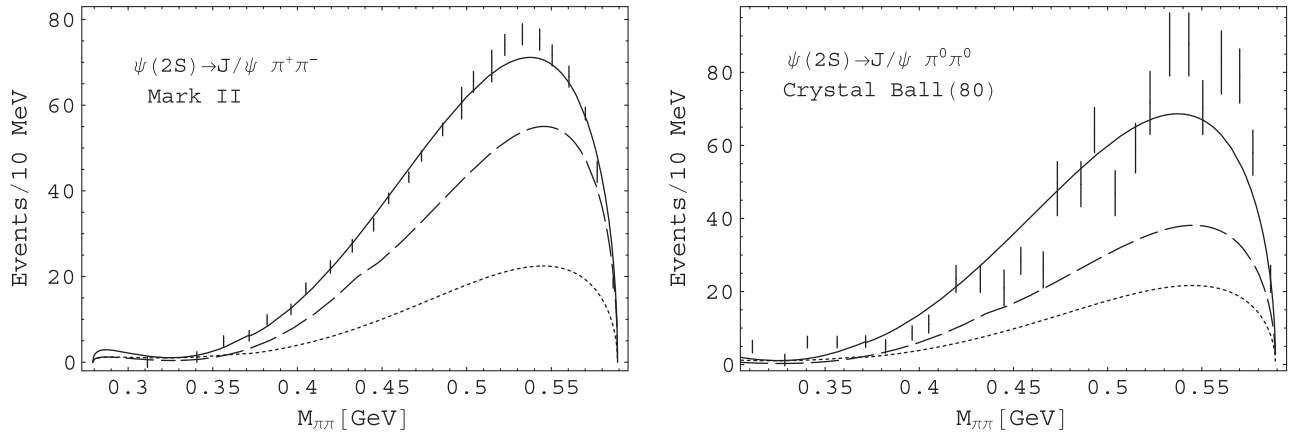


FIG. 3. The decays $\psi(2S) \rightarrow J/\psi(\pi^+ \pi^-, \pi^0 \pi^0)$. The solid, dotted and dashed lines as explained in Fig. 1.

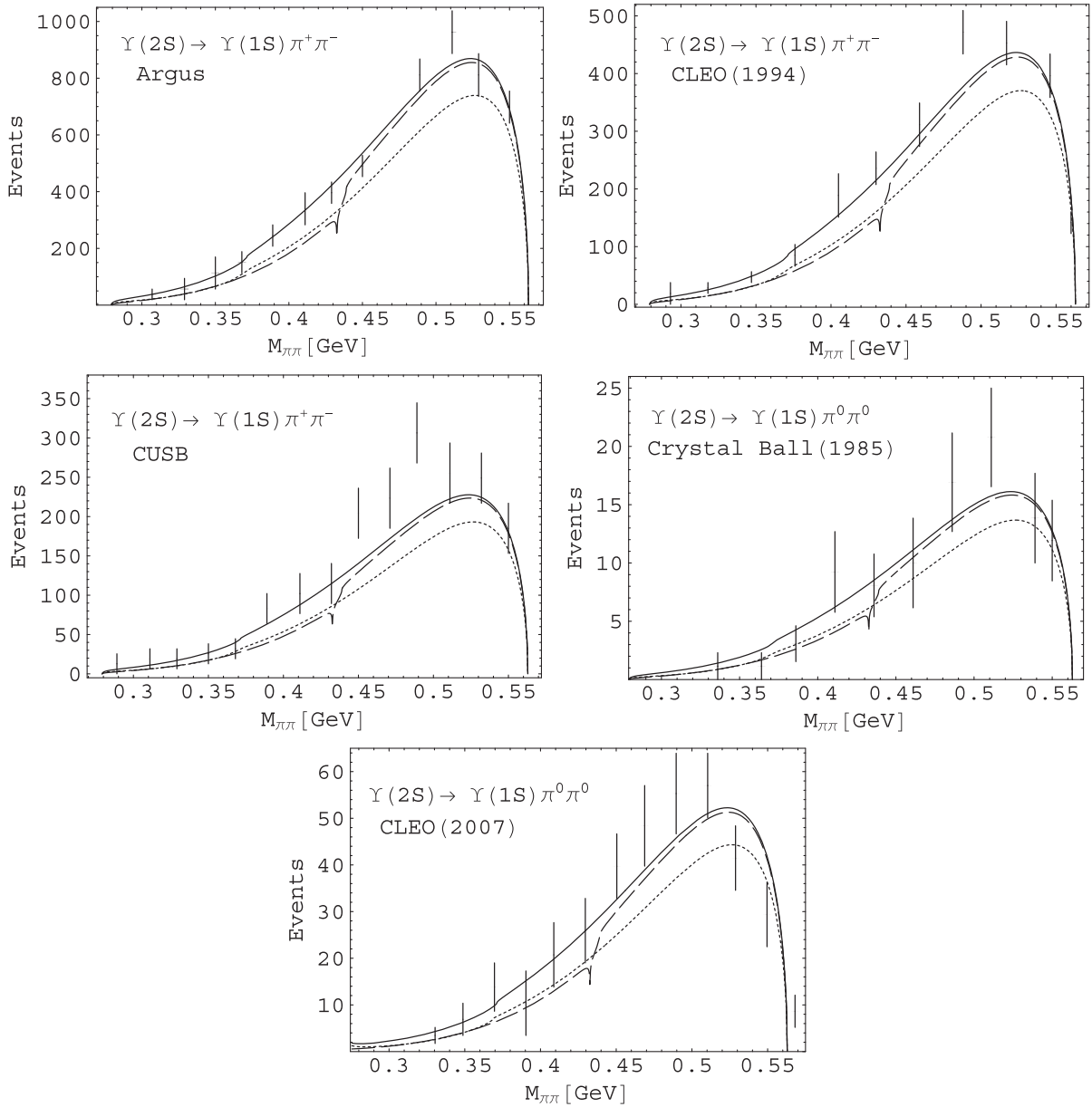


FIG. 4. The decays $Y(2S) \rightarrow Y(1S)(\pi^+ \pi^-, \pi^0 \pi^0)$. The solid, dotted and dashed lines as explained in Fig. 1.

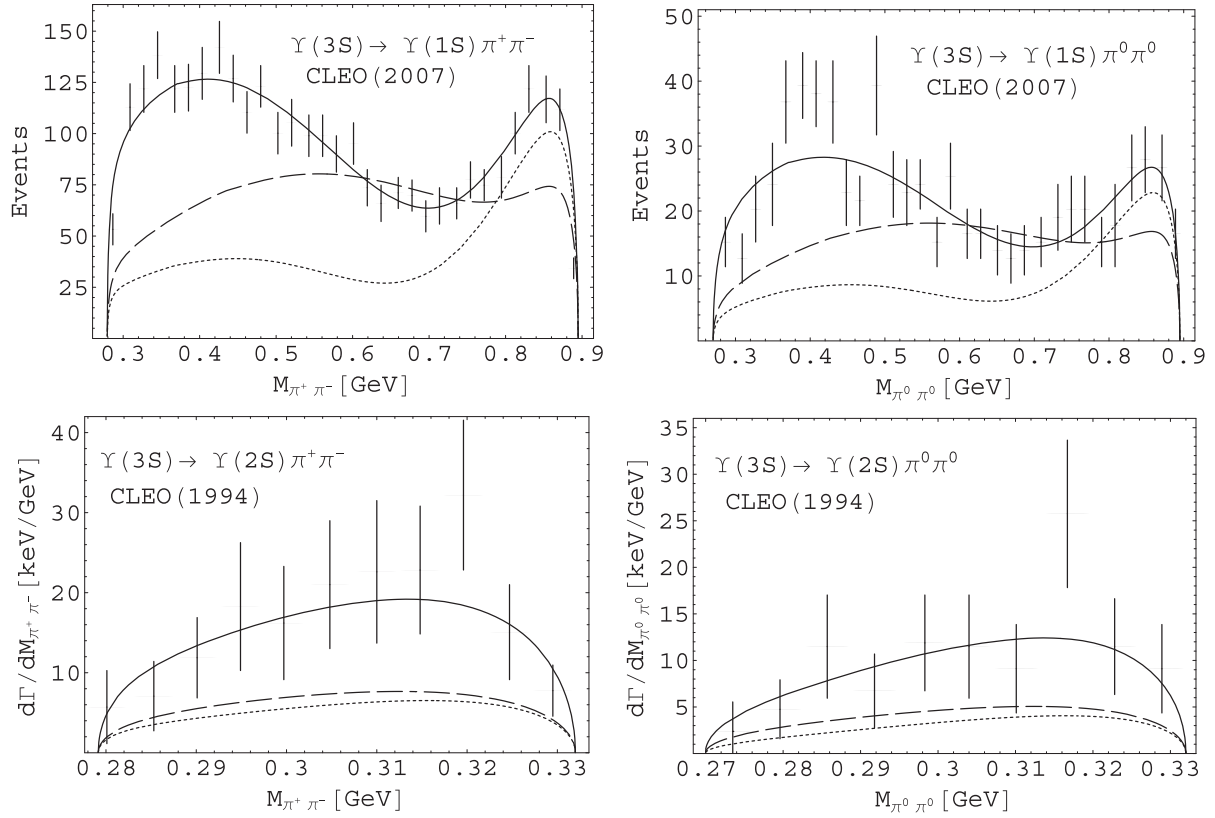


FIG. 5. The decays $\Upsilon(3S) \rightarrow \Upsilon(1S)(\pi^+\pi^-, \pi^0\pi^0)$ (upper panel) and $\Upsilon(3S) \rightarrow \Upsilon(2S)(\pi^+\pi^-, \pi^0\pi^0)$ (lower panel). The solid, dotted and dashed lines as explained in Fig. 1.

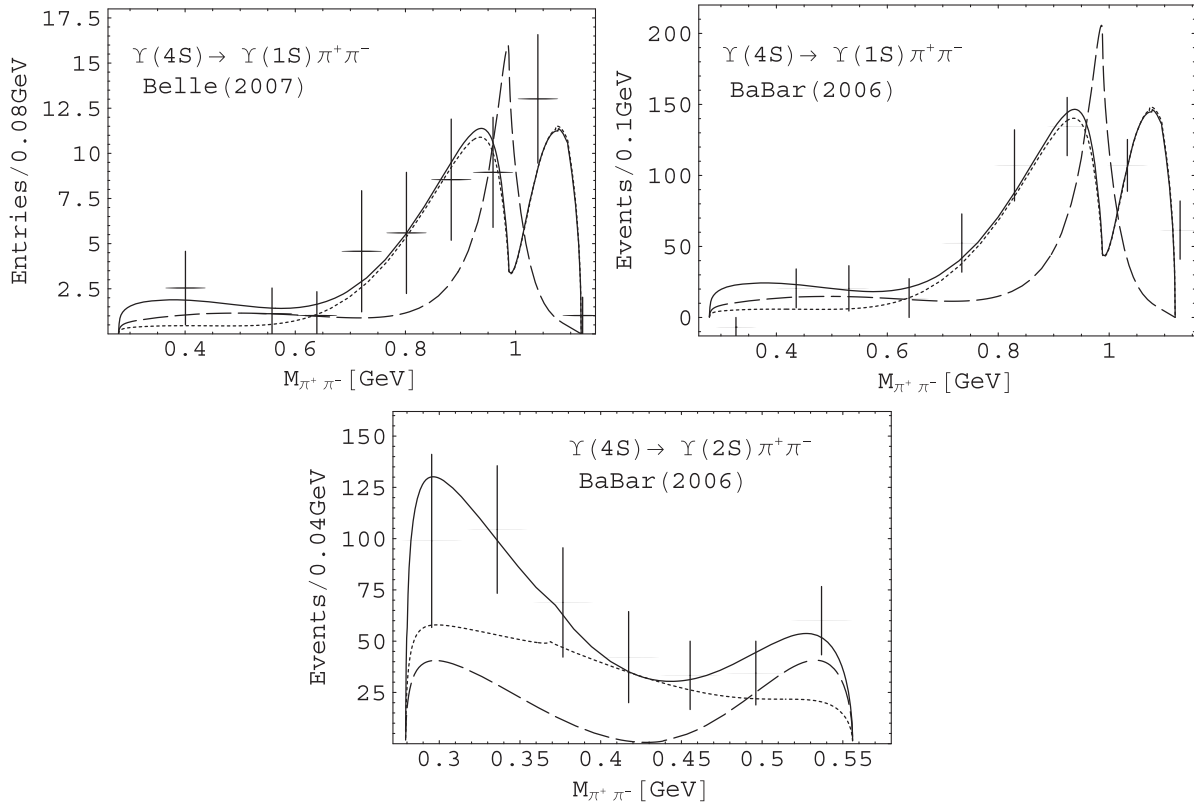


FIG. 6. The decays $\Upsilon(4S) \rightarrow \Upsilon(1S, 2S)\pi^+\pi^-$. The solid, dotted and dashed lines as explained in Fig. 1.

1.39, for $\Upsilon(5S) \rightarrow \Upsilon(2S)(\pi^+\pi^-, \pi^0\pi^0)$, $\chi^2/\text{ndf} \approx 1.10$, for $\Upsilon(5S) \rightarrow \Upsilon(3S)(\pi^+\pi^-, \pi^0\pi^0)$, $\chi^2/\text{ndf} \approx 0.87$.

The free parameters in Eqs. (1)–(4), depending on the couplings of J/ψ , $\psi(2S)$ and the $\Upsilon(mS)$ to the channels $\pi\pi$, $K\bar{K}$ and $\eta\eta$, are found to be $\alpha_2 = 0.1729 \pm 0.011$, $\beta_2 = -0.0438 \pm 0.027$, $\gamma_{10} = 0.8807 \pm 0.023$, $\gamma_{11} = 1.0524 \pm 0.016$, $\gamma_{20} = -2.1591 \pm 0.029$, $\gamma_{21} = 0.1419 \pm 0.030$, $\gamma_{30} = 3.0636 \pm 0.017$, $\gamma_{31} = -2.6181 \pm 0.018$, $\delta_{10} = 0.5054 \pm 0.011$, $\delta_{11} = 9.2480 \pm 0.072$, $\delta_{20} = 6.0865 \pm 0.087$, $\delta_{21} = -57.1203 \pm 1.890$, $\delta_{30} = -5.1795 \pm 0.032$, $\delta_{31} = 2.6004 \pm 0.027$, $\rho_{10}^{(21)} = 0.5117 \pm 0.013$, $\rho_{11}^{(21)} = 46.1651 \pm 0.656$, $\rho_{20}^{(21)} = 0.6397 \pm 0.043$, $\rho_{21}^{(21)} = -21.6599 \pm 0.972$, $\rho_{30}^{(21)} = 9.0577 \pm 0.054$, $\rho_{31}^{(21)} = -6.3357 \pm 0.034$,

$\rho_{10}^{(31)} = 0.9728 \pm 0.026$, $\rho_{11}^{(31)} = -2.4287 \pm 0.023$, $\rho_{20}^{(31)} = 0.9164 \pm 0.041$, $\rho_{21}^{(31)} = 0.5073 \pm 0.017$, $\rho_{30}^{(31)} = 0.2223 \pm 0.017$, $\rho_{31}^{(31)} = -0.7330 \pm 0.021$, $\rho_{10}^{(32)} = 0.0274 \pm 0.010$, $\rho_{11}^{(32)} = 56.4752 \pm 1.770$, $\rho_{20}^{(32)} = 1.6553 \pm 0.027$, $\rho_{21}^{(32)} = -50.5964 \pm 2.600$, $\rho_{30}^{(32)} = 16.1394 \pm 0.870$, $\rho_{31}^{(32)} = -55.0251 \pm 2.130$, $\rho_{10}^{(41)} = 0.4889 \pm 0.012$, $\rho_{11}^{(41)} = -2.4299 \pm 0.057$, $\rho_{20}^{(41)} = -0.8203 \pm 0.041$, $\rho_{21}^{(41)} = 0.0583 \pm 0.012$, $\rho_{30}^{(41)} = -0.0791 \pm 0.011$, $\rho_{31}^{(41)} = 0.0542 \pm 0.003$, $\rho_{10}^{(42)} = 2.5852 \pm 0.066$, $\rho_{11}^{(42)} = -8.7188 \pm 0.177$, $\rho_{20}^{(42)} = 1.7985 \pm 0.059$, $\rho_{21}^{(42)} = -9.7334 \pm 0.790$, $\rho_{30}^{(42)} = 0.6851 \pm 0.019$, $\rho_{31}^{(42)} = 0.9233 \pm 0.035$, $\rho_{10}^{(51)} = -1.1574 \pm$

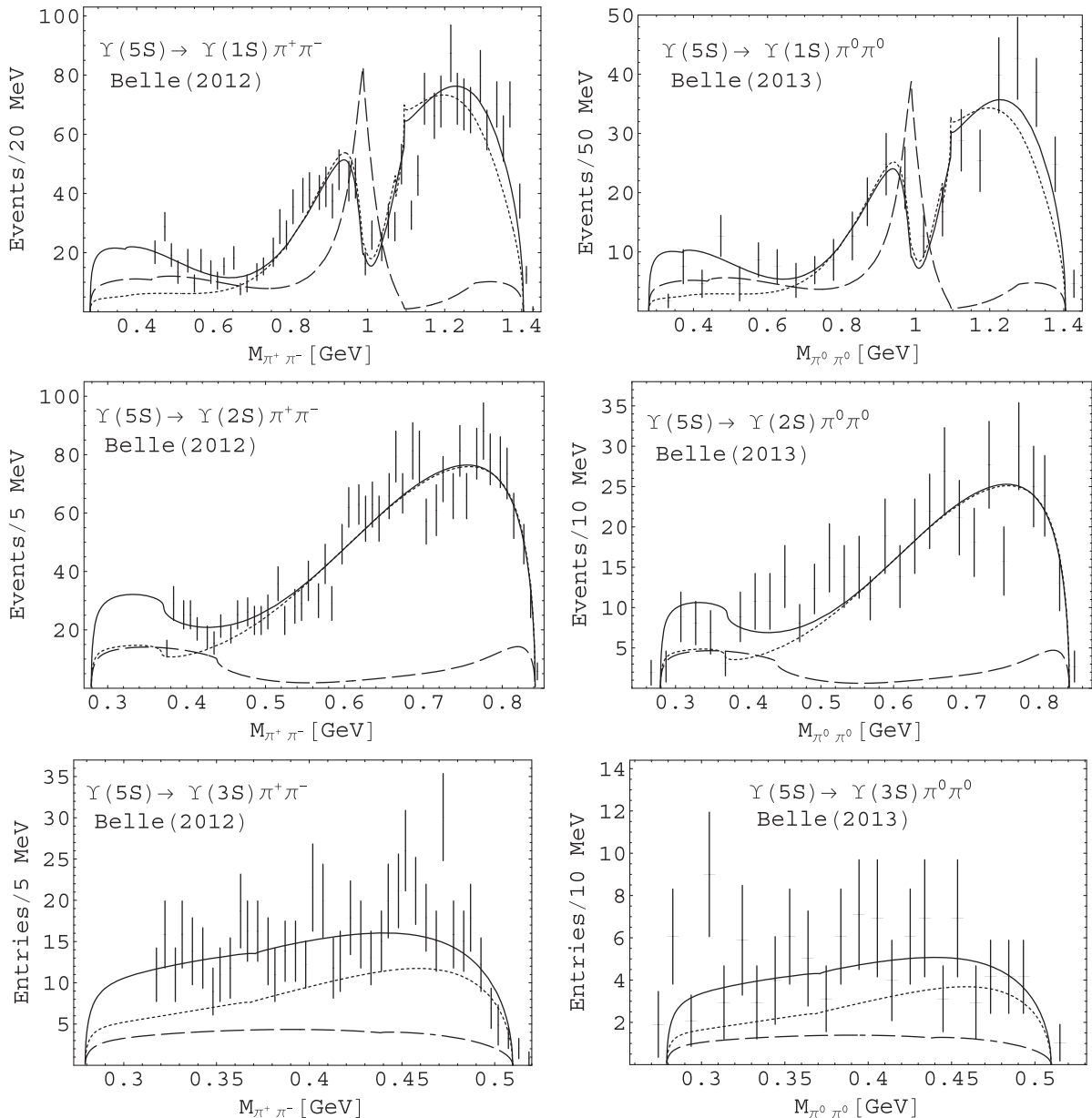


FIG. 7. The decays and $\Upsilon(5S) \rightarrow \Upsilon(ns)(\pi^+\pi^-, \pi^0\pi^0)$ ($n = 1, 2, 3$). The solid, dotted and dashed lines as explained in Fig. 1.

0.057, $\rho_{11}^{(51)} = 5.1800 \pm 0.221$, $\rho_{20}^{(51)} = 3.7654 \pm 0.033$,
 $\rho_{21}^{(51)} = -4.7934 \pm 0.834$, $\rho_{30}^{(51)} = -3.0899 \pm 0.054$, $\rho_{31}^{(51)} =$
 1.9762 ± 0.065 , $\rho_{10}^{(52)} = 1.2657 \pm 0.063$, $\rho_{11}^{(52)} = 1.4487 \pm$
 0.071 , $\rho_{20}^{(52)} = -1.3707 \pm 0.057$, $\rho_{21}^{(52)} = 2.2858 \pm 0.770$,
 $\rho_{30}^{(52)} = -5.6127 \pm 0.041$, $\rho_{31}^{(52)} = 10.6278 \pm 1.120$, $\rho_{10}^{(53)} =$
 1.0362 ± 0.016 , $\rho_{11}^{(53)} = 1.8643 \pm 0.047$, $\rho_{20}^{(53)} = 0.6141 \pm$

0.023, $\rho_{21}^{(53)} = 0.1688 \pm 0.063$, $\rho_{30}^{(53)} = -0.5437 \pm 0.019$,
 $\rho_{31}^{(53)} = 0.3827 \pm 0.071$.

In Figs. 2–7 we shown our fits to the decay data. In all next figures the solid lines, as above, correspond to contribution of all relevant f_0 -resonances; the dotted, of the $f_0(500)$, $f_0(980)$, and $f'_0(1500)$; the dashed, of the $f_0(980)$ and $f'_0(1500)$.

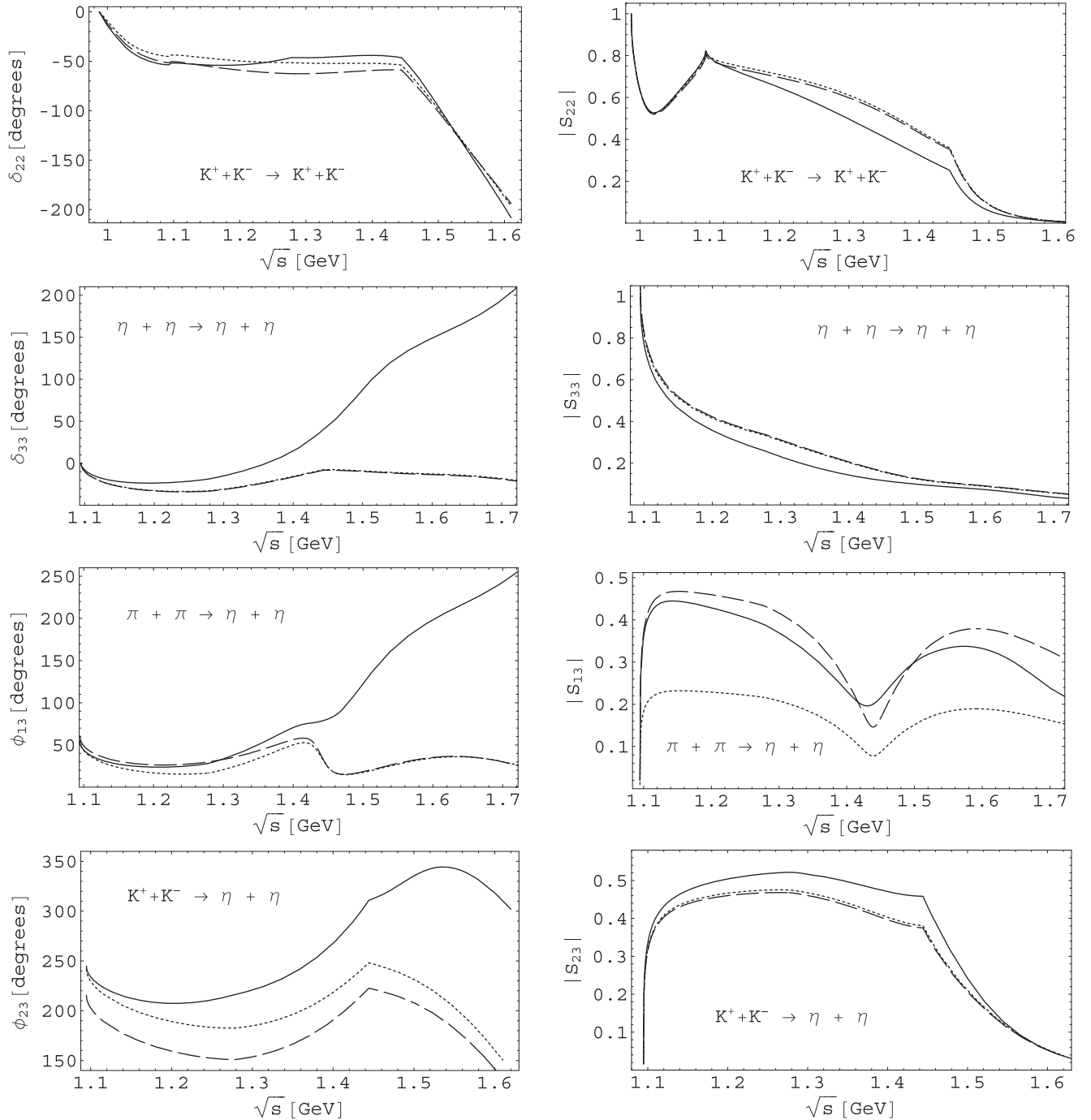


FIG. 8. The phase shifts and moduli of the S-matrix element in the S-wave $K\bar{K}$ and $\eta\eta$ scattering (two upper panels), in $\pi\pi \rightarrow \eta\eta$ (third panel), and in $K\bar{K} \rightarrow \eta\eta$ (lower panel). The solid, dotted and dashed lines as explained in Fig. 1.

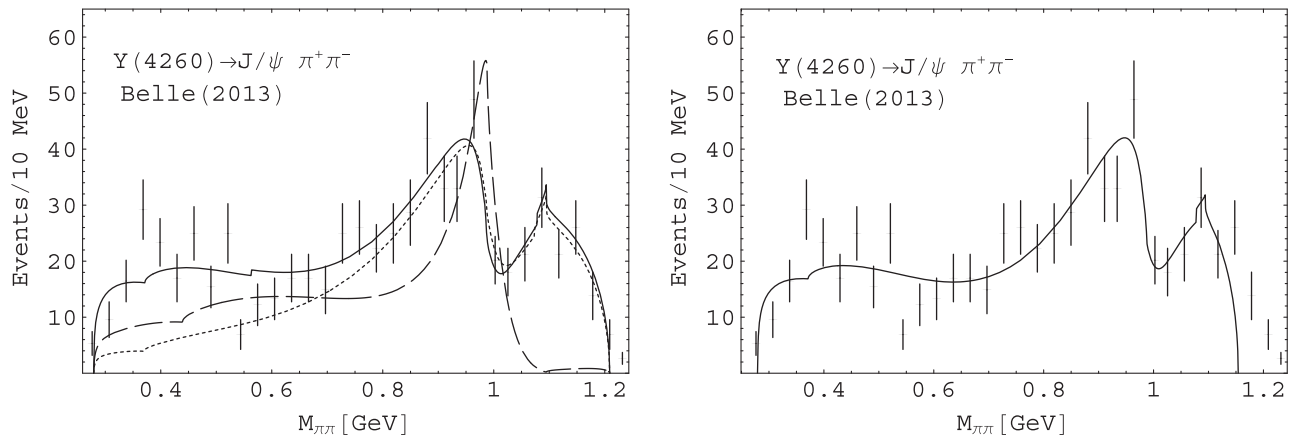


FIG. 9. The decay $Y(4260) \rightarrow J/\psi \pi^+ \pi^-$. The solid, dotted and dashed lines as explained in Fig. 1. The data are taken from Ref. [28].

Taking into account success in describing the multi-channel $\pi\pi$ scattering and the above-shown decays of charmonia and bottomonia, it is worth to show obtained predictions for amplitudes of the $\eta\eta$ and $K\bar{K}$ scattering and of the transitions $\eta\eta \rightarrow \pi\pi$ and $\eta\eta \rightarrow K\bar{K}$ which are used in our calculations and almost or entirely unknown from experiment (Fig. 8). In the Appendix we show formulas for the phase shifts and moduli of indicated amplitudes which were used also at calculating decays of charmonia and bottomonia.

Finally, we have applied our method for describing the data on the decay of charmonium $X(4260)$ (sometimes is indicated as $Y(4260)$) to $J/\psi \pi^+ \pi^-$ [28]. There was used the formula analogous Eq. (3), and the obtained description is quite satisfactory: $\chi^2/\text{ndf} \approx 1.23$ and fitting to the data shown on Fig. 9. The general combined description of all considered processes is obtained with the total $\chi^2/\text{ndf} = 764.417/(739 - 119) \approx 1.31$. In the PDG tables [21] for the state $X(4260)$ one indicates the quantum numbers $I^G(J^{PC}) = ?^?(1^{--})$ and the mass $m = 4251 \pm 9$ MeV. However, this analysis shows that the data [28] correspond to the decay of charmonium with the mass 4.3102 GeV (left-hand picture), not with 4.251 GeV (right-hand one on Fig. 9). Furthermore, since we have shown that the basic forms of the dipion mass spectra of charmonia and bottomonia pion-pion transitions are explained by the unified mechanism, one can think that characteristic pictures of the mass spectra of analogous charmonia and bottomonia transitions are similar, of course, with taking into account distortions due to the phase space volume. Obviously, for justification of this assumption there is important the spectator role of vector meson in the final state. Furthermore, to some extent this assumption is supported by comparison of the corresponding experimental data: cf. Figs. 3 and 4 for $\psi(2S) \rightarrow J/\psi(1S)(\pi^+ \pi^-, \pi^0 \pi^0)$ and $\Upsilon(2S) \rightarrow \Upsilon(1S)(\pi^+ \pi^-, \pi^0 \pi^0)$, respectively. Further one can see that the basic forms of

dipion mass spectra of the decay $\Upsilon(4S) \rightarrow \Upsilon(1S)\pi^+ \pi^-$ (Fig. 6, two left-hand pictures from above) and of the charmonium $X(4260)$ (Fig. 9) are similar. This can be some indication that the $X(4260)$ is a third radial excitation, i.e., the 4S state with the mass 4.3102 GeV. The obtained parameters in equation of type (3), which depend on the couplings of $X(2S)(4310)$ to the channels $\pi\pi$, $K\bar{K}$ and $\eta\eta$, are $\delta_{10}^{(41)} = 0.0062$, $\delta_{11}^{(41)} = 3.6752$, $\delta_{10}^{(41)} = 4.1488$, $\delta_{11}^{(41)} = -2.7138$, $\delta_{10}^{(41)} = -6.2914$, $\delta_{11}^{(41)} = 5.5438$. N (normalization to experiment) in Eq. (9) is 0.3567.

III. CONCLUSIONS AND DISCUSSION

The combined analysis was performed for data on isoscalar S-wave processes $\pi\pi \rightarrow \pi\pi, K\bar{K}, \eta\eta$ and on the decays of the charmonia— $J/\psi \rightarrow \phi(\pi\pi, K\bar{K})$, $\psi(2S) \rightarrow J/\psi \pi\pi$, $Y(4260) \rightarrow J/\psi \pi^+ \pi^-$ —and of the bottomonia— $\Upsilon(mS) \rightarrow \Upsilon(nS)\pi\pi$ ($m > n$, $m = 2, 3, 4, 5$, $n = 1, 2, 3$) from the ARGUS, Crystal Ball, CLEO, CUSB, DM2, Mark II, Mark III, BES II, BABAR, and Belle Collaborations.

It is shown that the dipion and $K\bar{K}$ mass spectra in the above-indicated decays of charmonia and the dipion mass spectra of bottomonia are explained by the unified mechanism which is based on our previous conclusions on wide resonances [5,6] and is related to contributions of the $\pi\pi$, $K\bar{K}$ and $\eta\eta$ coupled channels including their interference. It is shown that in the final states of these decays (except $\pi\pi$ scattering) the contribution of coupled processes, e.g., $K\bar{K}, \eta\eta \rightarrow \pi\pi$, is important even if these processes are energetically forbidden.

When analyzing the decay $Y(4260) \rightarrow J/\psi \pi^+ \pi^-$, it is obtained some indication that the charmonium $X(4260)$, the dipion spectrum of $J/\psi \pi^+ \pi^-$ decay of which is published in Ref. [28], is a third radial excitation, i.e., the 4S state with the mass 4.3102 GeV.

The allowance for the effect of the $\eta\eta$ channel in the considered decays both kinematically (i.e., via the uniformizing variable) and also by adding the $\pi\pi \rightarrow \eta\eta$ amplitude in the formulas for the decays permits us to eliminate unphysical (i.e., those related with no channel thresholds) nonregularities in some $\pi\pi$ distributions, being present without this extension of the description [3], obtaining a reasonable and satisfactory description of all considered $\pi\pi$ and $K\bar{K}$ spectra in the two-pion and $K\bar{K}$ transitions of charmonia and in the two-pion transitions of bottomonia.

It was also very useful to consider the role of individual f_0 resonances in contributions to the dipion mass distributions in the indicated decays. For example, it is seen that the sharp dips about 1 GeV in the $\Upsilon(4S, 5S) \rightarrow \Upsilon(1S)\pi^+\pi^-$ decays are related with the $f_0(500)$ contribution to the interfering amplitudes of $\pi\pi$ scattering and $K\bar{K}, \eta\eta \rightarrow \pi\pi$ processes. Namely the consideration of this role of the $f_0(500)$ allows us to make conclusion on the existence of the sharp dip about 1 GeV in the dipion mass spectrum of the $\Upsilon(4S) \rightarrow \Upsilon(1S)\pi^+\pi^-$ decay where, unlike $\Upsilon(5S) \rightarrow \Upsilon(1S)\pi^+\pi^-$, the scarce data do not permit to do that conclusion yet.

Also, a manifestation of the $f_0(1370)$ is turned out to be interesting and unexpected. First, in the satisfactory description of the $\pi\pi$ spectrum of decay $J/\psi \rightarrow \phi\pi\pi$, the second large peak in the 1.4-GeV region can be naively imagined as related to the contribution of the $f_0(1370)$. We have shown that this is not right—the constructive interference between the contributions of the $\eta\eta$ and $\pi\pi$ and $K\bar{K}$ channels plays the main role in formation of the 1.4-GeV peak. This is quite in agreement with our earlier conclusion that the $f_0(1370)$ has a dominant $s\bar{s}$ component [5].

On the other hand, it turned out that the $f_0(1370)$ contributes considerably in the near- $\pi\pi$ -threshold region of many dipion mass distributions, especially making the threshold bell-shaped form of the dipion spectra in the decays $\Upsilon(mS) \rightarrow \Upsilon(nS)\pi\pi$ ($m > n, m=3,4,5, n=1, 2, 3$). This fact, first, confirms existence of the $f_0(1370)$ (up to now there is no firm conviction if it exists or not). Second, that exciting role of this meson in making the threshold bell-shaped form of the dipion spectra can be explained as follows: the $f_0(1370)$, being predominantly the $s\bar{s}$ state [6] and practically not contributing to the $\pi\pi$ -scattering amplitude, influences noticeably the $K\bar{K}$ scattering; e.g., it was shown that the $K\bar{K}$ -scattering length is very sensitive to whether this state does exist or not [27]. The interference of contributions of the $\pi\pi$ -scattering amplitude and the analytically-continued $\pi\pi \rightarrow K\bar{K}$ and $\pi\pi \rightarrow \eta\eta$ amplitudes leads to the observed results.

It is important that we have performed a combined analysis of available data on the processes $\pi\pi \rightarrow \pi\pi, K\bar{K}, \eta\eta$, on above-indicated decays of charmonia and bottomonia with the data from many collaborations. The convincing description (when including also the $\eta\eta$ channel) of the mentioned processes confirmed all our previous conclusions on the unified mechanism of formation of the basic dipion and $K\bar{K}$ spectra, which is based on our previous conclusions on wide resonances [5,6] and is related to contributions of the $\pi\pi, K\bar{K}$ and $\eta\eta$ coupled channels including their interference. This also confirmed all our earlier results on the scalar mesons [6]; the most important results are

- (1) Confirmation of the $f_0(500)$ with a mass of about 700 MeV and a width of 930 MeV (the pole position on sheet II is $514.5 \pm 12.4 - 465.6 \pm 5.9$ MeV).
- (2) An indication that the $f_0(980)$ (the pole on sheet II is $1008.1 \pm 3.1 - i(32.0 \pm 1.5)$ MeV) is a non- $q\bar{q}$ state.
- (3) An indication for the $f_0(1370)$ and $f_0(1710)$ to have a dominant $s\bar{s}$ component.
- (4) An indication for the existence of two states in the 1500-MeV region: the $f_0(1500)$ ($m_{\text{res}} \approx 1495$ MeV, $\Gamma_{\text{tot}} \approx 124$ MeV) and the $f'_0(1500)$ ($m_{\text{res}} \approx 1539$ MeV, $\Gamma_{\text{tot}} \approx 574$ MeV).

ACKNOWLEDGMENTS

This work was supported in part by the Heisenberg-Landau Program, by the Votruba-Blokhintsev Program for Cooperation of Czech Republic with JINR, by the Grant Agency of the Czech Republic (Grant No. P203/15/04301), by the Grant Program of Plenipotentiary of Slovak Republic at JINR, by the Bogoliubov-Infeld Program for Cooperation of Poland with JINR, by the BMBF (Projects No. 05P2015, BMBF-FSP 202), by CONICYT (Chile) PIA/Basal FB0821, by Tomsk State University Competitiveness Improvement Program, by the Russian Federation program “Nauka”(Contract No. 0.1764.GZB.2017), by Tomsk Polytechnic University Competitiveness Enhancement Program (Grant No. VIU-FTI-72/2017), and by the Polish National Science Center (NCN) Grant No. DEC-2013/09/B/ST2/04382.

APPENDIX: PHASE SHIFTS AND MODULI-PARAMETERS OF THE TWO-MESON FINAL-STATE RE-SCATTERING AMPLITUDE

The elements of S -matrix for 3-channel $\pi\pi$ scattering are represented via their moduli $\eta_{\alpha\alpha} = |S_{\alpha\alpha}|$, $\xi_{\alpha\beta} = |S_{\alpha\beta}|$ ($\alpha \neq \beta$) and phase shifts $\delta_{\alpha\alpha}$, $\phi_{\alpha\beta}$ ($\alpha, \beta = 1, 2, 3$) as follows:

$$S_{\alpha\alpha} = \eta_{\alpha\alpha} e^{2i\delta_{\alpha\alpha}}, \quad S_{\alpha\beta} = i\xi_{\alpha\beta} e^{i\phi_{\alpha\beta}} (\alpha \neq \beta). \quad (\text{A1})$$

The phase shifts in Eq. (A1) have the form:

$$\begin{aligned}\Phi_{11}(s) &= \arg(S_{11}^{\text{res}}(s)) + \pi + 2B_1(s), \\ B_1(s) &= \sqrt{\frac{s-s_1}{s_1}} \left(a_{11} + a_{1\sigma} \frac{s-s_\sigma}{s_\sigma} \theta(s-s_\sigma) + a_{1v} \frac{s-s_v}{s_v} \theta(s-s_v) \right), \\ \delta_{11}(s) &= \Phi_{11}(s) \theta(M_1^2 - s) + (\Phi_{11}(s) + 2\pi) \theta(s - M_1^2) \theta(M_3^2 - s) + (\Phi_{11}(s) + 4\pi) \theta(s - M_3^2),\end{aligned}\quad (\text{A2})$$

$$\begin{aligned}\Phi_{22}(s) &= \arg(S_{22}^{\text{res}}(s)) + 2B_2(s), \\ B_2(s) &= \sqrt{\frac{s-s_2}{s_2}} \left(a_{21} + a_{2\sigma} \frac{s-s_\sigma}{s_\sigma} \theta(s-s_\sigma) + a_{2v} \frac{s-s_v}{s_v} \theta(s-s_v) \right), \\ \delta_{22}(s) &= \Phi_{22}(s) \theta(M_{12}^2 - s) + \Phi_{22}(s) - 2\pi \theta(s - M_{12}^2) \theta(M_{13}^2 - s) + \Phi_{22}(s) \theta(s - M_{13}^2) \theta(M_{14}^2 - s) \\ &\quad + (\Phi_{22}(s) - 2\pi) \theta(s - M_{14}^2),\end{aligned}\quad (\text{A3})$$

$$\begin{aligned}\Phi_{33}(s) &= \arg(S_{33}^{\text{res}}(s)) + 2B_3(s), \\ B_3(s) &= \sqrt{\frac{s-s_3}{s_3}} \left(a_{31} + a_{1\sigma} \frac{s-s_\sigma}{s_\sigma} \theta(s-s_\sigma) + a_{3v} \frac{s-s_v}{s_v} \theta(s-s_v) \right), \\ \delta_{33}(s) &= \Phi_{33}(s) \theta(M_{15}^2 - s) + (\Phi_{33}(s) + 2\pi) \theta(s - M_{15}^2),\end{aligned}\quad (\text{A4})$$

$$\begin{aligned}\Phi_{12}(s) &= \arg(S_{12}^{\text{res}}(s)) + \pi + B_1(s) + B_2(s), \\ \phi_{12}(s) &= \Phi_{12}(s) \theta(M_2^2 - s) + (\Phi_{12}(s) + \pi) \theta(s - M_2^2) \theta(M_3^2 - s) + (\Phi_{12}(s) + 2\pi) \theta(s - M_3^2),\end{aligned}\quad (\text{A5})$$

$$\begin{aligned}\Phi_{13}(s) &= \arg(S_{13}^{\text{res}}(s)) + B_1(s) + B_3(s), \\ \phi_{13}(s) &= \Phi_{13}(s) \theta(M_6^2 - s) + (\Phi_{13}(s) + \pi) \theta(s - M_6^2),\end{aligned}\quad (\text{A6})$$

$$\begin{aligned}\Phi_{23}(s) &= \text{Re}[\arg(S_{23}^{\text{res}}(s)) + B_2(s) + B_3(s)] + \pi + 0.914406 \theta(s - s_3), \\ \phi_{23}(s) &= \Phi_{23}(s) \theta(M_7^2 - s) + (\Phi_{23}(s) + \pi) \theta(s - M_7^2) \theta(s_3 - s) + \Phi_{23}(s) \theta(s - s_3) \theta(M_8^2 - s) \\ &\quad + (\Phi_{23}(s) + \pi) \theta(s - M_8^2) \theta(M_9^2 - s) + (\Phi_{23}(s) - \pi) \theta(s - M_9^2) \theta(M_{10}^2 - s) \\ &\quad + \Phi_{23}(s) \theta(s - M_{10}^2) \theta(M_{11}^2 - s) + (\Phi_{23}(s) + \pi) \theta(s - M_{11}^2),\end{aligned}\quad (\text{A7})$$

where $M_1 = 1.0003704$, $M_2 = 1.1699$, $M_3 = 1.4355$, $M_4 = 0.5620973$, $M_5 = 1.6260221$, $M_6 = 1.4032403$, $M_7 = 1.0376107$, $M_8 = 1.1946199$, $M_9 = 1.3788410$, $M_{10} = 1.4356518$, $M_{11} = 1.5349385$, $M_{12} = 1.17160511$, $M_{13} = 1.32724876$, $M_{14} = 1.51411720$, $M_{15} = 1.48837285$; $a_{11} = 0.0$, $a_{1\sigma} = 0.0199$, $a_{1v} = 0.0$, $a_{21} = -2.4649$, $a_{2\sigma} = -2.3222$, $a_{2v} = -6.611$, $a_{31} = -0.37755$, $a_{3\sigma} = 0.8209$, $a_{3v} = -2.74575$; $s_\sigma = 1.6338 \text{ GeV}^2$, $s_v = 2.0857 \text{ GeV}^2$. The values of energies M_i and M_{jk} , at which the corresponding phases possess discontinuities corrected by adding an appropriate multiple of 90° , are determined empirically and relate to the used experimental data.

The resonance parts of S -matrix elements $S_{ij}^{\text{res}}(s)$ are parametrized by poles and zeros, representing resonances, with using the Le Couteur–Newton relations which in the 3-channel case and on the w -plane are shown in our work [5]. For calculation of moduli of the S -matrix elements there are needed also their inelastic background parts:

$$S_{ii}^{\text{bgr}} = \exp \left\{ -2\theta(s - s_i) \sqrt{\frac{s - s_i}{s_i}} \left(b_{i1} + b_{i\sigma} \frac{s - s_\sigma}{s_\sigma} \theta(s - s_\sigma) + b_{iv} \frac{s - s_v}{s_v} \theta(s - s_v) \right) \right\}, \quad (\text{A8})$$

$$S_{ij}^{\text{bgr}} = \sqrt{S_{ii}^{\text{bgr}} S_{jj}^{\text{bgr}}} \quad (i < j), \quad (\text{A9})$$

where $b_{11} = b_{1\sigma} = 0.0$, $b_{1v} = 0.0338$, $b_{21} = b_{2\sigma} = 0.0$, $b_{2v} = 7.073$, $b_{31} = 0.6421$, $b_{3\sigma} = 0.4851$, $b_{3v} = 0.0$.

- [1] Yu. A. Simonov and A. I. Veselov, *Phys. Rev. D* **79**, 034024 (2009).
- [2] Yu. S. Surovtsev, P. Bydžovský, T. Gutsche, R. Kamiński, V. E. Lyubovitskij, and M. Nagy, *Phys. Rev. D* **91**, 037901 (2015).
- [3] Yu. S. Surovtsev, P. Bydžovský, T. Gutsche, R. Kamiński, V. E. Lyubovitskij, and M. Nagy, *Phys. Rev. D* **92**, 036002 (2015).
- [4] Yu. S. Surovtsev, P. Bydžovský, R. Kamiński, V. E. Lyubovitskij, and M. Nagy, *Phys. Rev. D* **86**, 116002 (2012).
- [5] Yu. S. Surovtsev, P. Bydžovský, V. E. Lyubovitskij, R. Kamiński, and M. Nagy, *J. Phys. G Nucl. Part. Phys.* **41**, 025006 (2014).
- [6] Yu. S. Surovtsev, P. Bydžovský, R. Kamiński, V. E. Lyubovitskij, and M. Nagy, *Phys. Rev. D* **89**, 036010 (2014).
- [7] Yu. S. Surovtsev, P. Bydžovský, T. Gutsche, V. E. Lyubovitskij, R. Kamiński, and M. Nagy, *Nucl. Phys. B* **245**, 259 (2013).
- [8] M. Oreglia *et al.* (Crystal Ball Collaboration), *Phys. Rev. Lett.* **45**, 959 (1980).
- [9] A. Falvard *et al.* (DM2 Collaboration), *Phys. Rev. D* **38**, 2706 (1988).
- [10] G. Gidal *et al.* (Mark II Collaboration), *Phys. Lett. B* **107**, 153 (1981).
- [11] W. Lockman (Mark III Collaboration), *Proc. Hadron'89 Conference*, edited by F. Binon *et al.* (Editions Frontières, Gif-sur-Yvette, 1989), p. 109.
- [12] M. Ablikim *et al.*, *Phys. Lett. B* **607**, 243 (2005).
- [13] H. Albrecht *et al.* (ARGUS Collaboration), *Phys. Lett.* **134B**, 137 (1984).
- [14] D. Besson *et al.* (CLEO Collaboration), *Phys. Rev. D* **30**, 1433 (1984).
- [15] V. Fonseca *et al.* (CUSB Collaboration), *Nucl. Phys.* **B242**, 31 (1984).
- [16] D. Gelfman *et al.* (Crystal Ball Collaboration), *Phys. Rev. D* **32**, 2893 (1985).
- [17] A. Sokolov *et al.* (Belle Collaboration), *Phys. Rev. D* **75**, 071103 (2007); A. Bondar *et al.* (Belle Collaboration), *Phys. Rev. Lett.* **108**, 122001 (2012).
- [18] B. Aubert *et al.* (BABAR Collaboration), *Phys. Rev. Lett.* **96**, 232001 (2006).
- [19] K. J. Le Couteur, *Proc. R. London, Ser. A* **256**, 115 (1960); R. G. Newton, *J. Math. Phys.* **2**, 188 (1961); M. Kato, *Ann. Phys. (N.Y.)* **31**, 130 (1965).
- [20] Yu. S. Surovtsev, P. Bydžovský, and V. E. Lyubovitskij, *Phys. Rev. D* **85**, 036002 (2012).
- [21] C. Patrignani *et al.* (Particle Data Group Collaboration), *Chin. Phys. C* **40**, 100001 (2016).
- [22] D. Cronin-Hennessy *et al.* (CLEO Collaboration), *Phys. Rev. D* **76**, 072001 (2007).
- [23] F. Butler *et al.* (CLEO Collaboration), *Phys. Rev. D* **49**, 40 (1994).
- [24] P. Krokovny *et al.* (Belle Collaboration), *Phys. Rev. D* **88**, 052016 (2013).
- [25] D. Morgan and M. R. Pennington, *Phys. Rev. D* **48**, 1185 (1993).
- [26] D. Krupa, V. A. Meshcheryakov, and Yu. S. Surovtsev, *Nuovo Cimento A* **109A**, 281 (1996).
- [27] Yu. S. Surovtsev, D. Krupa, and M. Nagy, *Eur. Phys. J. A* **15**, 409 (2002); *Czech. J. Phys.* **56**, 807 (2006).
- [28] Z. Q. Liu *et al.* (Belle Collaboration), *Phys. Rev. Lett.* **110**, 252002 (2013).